HHS Public Access

Author manuscript

J Photochem Photobiol B. Author manuscript; available in PMC 2017 July 01.

Published in final edited form as:

J Photochem Photobiol B. 2016 July ; 160: 72–78. doi:10.1016/j.jphotobiol.2016.03.047.

The optical properties of mouse skin in the visible and near infrared spectral regions

Caetano P. Sabino[1,2], **Alessandro M. Deana**[3], **Tania M. Yoshimura**[1], **Daniela F. T. da Silva**[3], **Cristiane M. França**[3], **Michael R. Hamblin**[4,5,6], and **Martha S. Ribeiro**[1,*]

[1]Center for Lasers and Applications, Nuclear and Energy Research Institute, IPEN–CNEN/SP, São Paulo, SP, Brazil

[2]Institute for Biomedical Sciences, USP, São Paulo, SP, Brazil

[3]Biophotonics Post-Graduation Program, Universidade Nove de Julho, São Paulo, SP, Brazil

[4]Wellman Center for Photomedicine, Massachusetts General Hospital, Boston, MA, USA

[5]Department of Dermatology, Harvard Medical School, Boston, MA, USA

[6]Harvard-MIT Division of Health Sciences and Technology, Cambridge, MA, USA

Abstract

Visible and near-infrared radiation is now widely employed in health science and technology. Pre-clinical trials are still essential to allow appropriate translation of optical methods into clinical practice. Our results stress the importance of considering the mouse strain and gender when planning pre-clinical experiments that depend on light-skin interactions. Here, we evaluated the optical properties of depilated albino and pigmented mouse skin using reproducible methods to determine parameters that have wide applicability in biomedical optics. Light penetration depth (δ), absorption (μ_a), reduced scattering (μ'_s) and reduced attenuation (μ'_t) coefficients were calculated using the Kubelka-Munk model of photon transport and spectrophotometric measurements. Within a broad wavelength coverage (400–1400 nm), the main optical tissue interactions of visible and near infrared radiation could be inferred. Histological analysis was performed to correlate the findings with tissue composition and structure. Disperse melanin granules present in depilated pigmented mouse skin were shown to be irrelevant for light absorption. Gender mostly affected optical properties in the visible range due to variations in blood and abundance of dense connective tissue. On the other hand, mouse strains could produce more variations in the hydration level of skin, leading to changes in absorption in the infrared spectral region. A spectral region of minimal light attenuation, commonly referred as the “optical window”, was observed between 600 and 1350 nm.

Graphical abstract

*Corresponding Author: marthasr@usp.br, phone: 55-11-31339197, fax: 55-11-31339374.

Light-based technologies have been widely employed in health sciences. Since skin is the most common optical barrier in non-invasive techniques, its optical properties must be very well known. Our study investigated the light interaction with skin of bother genders from albino and pigmented strains. Our findings show a band of minimal light attenuation, referred as the “optical window”, between 600 and 1350 nm. Heme-containing proteins and water are main absorbing components in mouse skin, while melanin and fatty acids are minimally important. Gender mostly affects mouse skin optical properties in the visible range due to variations in blood and dense connective tissue abundance, while strains can introduce variations in the hydration level of skin, leading to absorption divergences in the infrared spectral region.

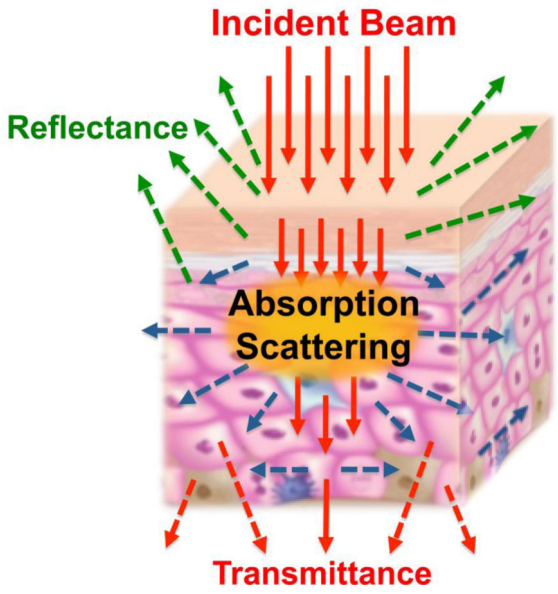

Keywords

biophotonics; tissue spectroscopy; skin optics; photodiagnosis; phototherapy; radiative transfer

1. Introduction

Over the last few decades, light has been widely employed in life sciences. [1] Specifically in medicine and dentistry, light has become a powerful alternative approach for non-invasive therapy and diagnosis.[2,3] Hence many pre-clinical studies employ light either for detection of pathology or to induce biological responses. There is a need to clearly understand light-tissue interactions as an important step before translation into clinical practice. [4] Mouse models have been widely employed in pre-clinical studies, even though the structure of mouse skin has some dissimilarities with human skin. Indeed, since many experimental approaches have first been tested in mice, some recent studies have explored the variation in the optical properties of mouse skin with respect to gender [5], strain and age [6], and pathological conditions, such as inflammatory processes.[7] Skin is the most important optical barrier in non-invasive optical techniques and in many cases it is the target tissue. Therefore, skin optics should be well characterized to optimize the use of light-based techniques.[8]

Theoretical approaches have not succeeded in achieving a satisfactory modelling approach for such a complex tissue, even though many models have been tested with varying degrees of success.[9] Kubelka-Munk (KM) photon transport theory is a simple, useful and well-accepted analytical model to provide a simple quantitative description of general tissue optics. It is a special case of the "many flux theory" describing two opposite distinguishable fluxes propagating in one dimension: one flux corresponding to the incident beam propagation, and the other to the resultant backscattering.[10,11] The main advantage of this model is its ability to be simply described by two differential equations, one corresponding to each flux, and the solutions are only dependent on the following parameters: sample thickness (D), the diffuse transmittance (T_d) and the reflectance (R_d). The light fluxes are subject to both elastic scattering and single photon absorption events and the probability of occurrence of these events is directly proportional to the KM scattering (S_{KM}) and absorption (A_{KM}) coefficients, respectively.

In the present work, we evaluated the optical behavior of freshly excised pieces of skin from male and female mice of two different strains: one albino strain (BALB/c) and another melanin pigmented strain (C57BL/6). Despite the fact that the melanin level is generally supposed to be low in C57BL/6 mice skin [6] it is recognized that skin pigmentation strongly influences the optical properties of tissues [12]. We analyzed a very broad spectral range (from 400 to 1400 nm), using the Kubelka-Munk model of photon transport and spectrophotometric measurements, to precisely describe the optical properties of mouse skin in terms of the optical coefficients μ_a, μ'_s, μ'_t and penetration depth (δ).

2. Materials & Methods

2.1. Animals

We used 4 to 6 weeks old healthy mice, 5 males and 5 females from each strain (C57BL/6 and BALB/c), for *ex vivo* skin sampling. Before the experiments, all animals were individually housed in acrylic plastic isolators in a 12 h light/dark cycle and fed with granulated food and water *ad libitum*. All animal procedures, care, and handling were carried out according to the ethical principles of animal experimentation formulated by the Brazilian College for Animal Experimentation (COBEA) and were approved – protocol 95/11 – by the local Ethics Committee on Animal Research and Care of IPEN/CNEN-SP.

Animals were euthanized by cervical dislocation, and hair excess on the dorsal region was carefully removed using an electric shaver. In order to minimize light interaction with any remaining fur, skin was depilated with a thioglycolate-based chemical (Veet Cream®, Reckitt Benckiser, Brazil). Samples were excluded if any sign of surface damage or inflammation was observable.

Samples were harvested from the dorsal region since this is a large region of skin with a homogenous structure, and is also the most frequently used region in mouse models. Skin from other regions such as the abdomen may have less homogeneous structures due to the presence of anatomical irregularities, appendages and other organs, such as mammary glands, that would negatively affect the precision of our interpretations. Skin pieces containing all tissue layers (*i.e.* from epidermis to subcutaneous tissue) of 2 x 2 cm were

then carefully detached from fascia and excised using surgical scissors. To provide mechanical support, each sample was positioned between two microscopy slides under minimal pressure as shown in Figure 1. Before the sample was positioned between the microscope glass slides, the epidermal surface was slightly moistened by a wet piece of cotton to minimize the effect of mismatched boundary conditions. Sample full thicknesses were measured by a hand caliper, subtracting the microscope slide thickness. To avoid possible artifacts due to sample compression or histological preparation, we used this thickness information to calculate the optical coefficients.

2.2. Spectroscopy analysis

Immediately after skin excision, spectroscopic measurements were carried out by a commercial spectrophotometer system (Cary 5000, Agilent, Australia) coupled to a single integrating sphere (Internal DRA-2500, Agilent, Australia). The spectra for transmittance and reflectance were measured at wavelengths ranging from 400 nm to 1400 nm. For experimental reproducibility, we avoided any sample folding and minimized the experimental time to avoid any sample deterioration due to possible dehydration and/or oxidation of tissue chromophores. Each measurement run took around 3 minutes of acquisition time. No tissue changes were visible after these measurements.

Transmittance measurements were obtained by placing the samples in front of the sample light beam (position “a”, in Figure 1) and the reflectance spectra were obtained by shifting the sample to position “b”. For total transmittance measurements we positioned samples on port “a”, and port “b” was closed to backscatter collimated transmittance. The sample beam was positioned at the center of the samples for reproducibility. During measurements, the rectangular sample beam dimensions were 1 cm high and <0.5 mm wide and the incident optical intensity <1 mW/cm^2. Any thermal effects were considered negligible.

Since the fresh skin samples were placed between two microscopy slides (Figure 1), the Fresnel reflection provided from the air/glass/water/glass/air interfaces were subtracted for position “a” and “b” in a baseline calibration. For baseline calibrations, we used two microscope slides with a thin layer of water between the slides.

The optical parameters A_{KM} and S_{KM} were determined using the one-dimensional, two-flux KM model. [10,13] The theoretical model provides rather simple mathematical formulations to extract the optical parameters from the measured values of T_d and R_d.

$$A_{\mathrm{KM}}=(x-1)S_{\mathrm{KM}} \quad (1)$$

$$S_{\mathrm{KM}}=\frac{1}{\mathrm{yD}}\ln\left[\frac{1-R_d(x-y)}{T_d}\right] \quad (2)$$

Where D [cm] is the sample thickness and:

$$x=\frac{1+R_d^2-T_d^2}{2R_d} \quad (3)$$

$$y=\sqrt{x^2-1} \quad (4)$$

The following equations were used to convert the KM coefficients into values of absorption coefficient (μ_a), reduced scattering coefficient (μ'_s), reduced attenuation coefficient (μ'_t) and penetration depth (5): [13.]

$$S_{\mathrm{KM}}=\frac{3}{4}\mu'_s \quad (5)$$

$$A_{\mathrm{KM}}=2\mu_a \quad (6)$$

$$\mu'_t=\mu_a+\mu'_s \quad (8)$$

$$\delta=[3\mu_a(\mu_a+\mu'_s)]^{-0.5} \quad (7)$$

2.3. Histological analysis

After spectroscopy, skin samples were fixed in 10 % buffered formaldehyde and routinely processed for hematoxylin and eosin histological staining. Separate measurements of epidermis, dermis, adipose tissue, muscle, and connective tissue were performed in three different areas of the images in a standardized manner using ImageJ for quantifications [14]. Additional sections were prepared and stained with Lillie Stain (all reagents from Sigma, St. Louis, MO, USA) which is specific for melanin.[15] Three images were obtained (Leica Microsystems, Wetzlar, Germany) from each skin sample. Lillie stain showed melanin granules as a dark blue color. The quantification of the area of melanin granules present in the skin was also performed using ImageJ Software.

2.4. Statistical analysis

For group comparison of melanin content in skin of pigmented mice, samples were found to have an approximated normal distribution (Shapiro–Wilks test) and to have homogeneous variances (Levene's test) thereby the unpaired t-Test was applied. To compare skin thickness among all groups, the *one-way* ANOVA test was used with Tukey post-hoc test. Groups for statistical analysis contained 5 independent measurements. Values are presented as averages

and standard error of the mean (SEM). Null hypotheses were rejected at lower than 0.05 significance level.

3. Results and discussion

The mean thicknesses of each layer of the skin tissue as quantified by histological analysis are presented in table 1. For our optical coefficient calculations, we used the total fresh skin sample thickness, measured by hand caliper, to provide an overall estimative of the optical coefficients. Skin sample thickness of BALB/c males was 750 ± 30 μm and that of females 520 ± 30 μm, while C57BL/6 males had a thickness of 540 ± 20 μm and females 540 ± 50 μm. As shown by the literature, female mice possess a more abundant adipose layer compared to males, who, on the other hand, had an overall thicker dermis and greater amount of subcutaneous tissue especially in the BALB/c strain. These sex-related skin-structure characteristics are also further inducible by administration of sex steroids or their respective inhibitors. [16] The epidermis and muscle layer thicknesses were statistically constant among the different groups.

The average diffuse transmittance and reflectance spectra of mice skin are presented in Figure 2. It was observed that male albino (BALB/c) mice had a lower transmittance and higher reflectance compared to other groups, especially between λ= 600 and 1300 nm. Albino males had a significantly thicker skin tissue due to a greater amount of connective tissue in the dermis (Table 1). Moreover, some differences can also be seen when comparing Figure 2a and Figure 2b regardless of gender and strain. The lower transmittance in the 400–600 nm band is related to light absorption by various chromophores combined with strong Rayleigh and Mie scattering, while beyond 950 nm water becomes a dominant chromophore.[11,12,17,18,19]

To discriminate between the influence of absorption and scattering, the optical coefficients are shown in Figure 3. In general, a few major absorption peaks (Figure 3a) were observed throughout the spectra, demonstrating the influence of the main chromophores in skin. The light-scattering properties of all groups were inversely proportional to wavelength, giving a decay rate that resembles a Rayleigh-Mie scattering curve (Figure 3b).

The absorption peaks centered at 425 nm and 552 nm are due to absorption by heme-containing proteins present in blood and muscle (Figure 3a). Oxyhemoglobin (O_2Hb) and deoxyhemoglobin (Hb), as well as oxymyoglobin (O_2Mb) and deoxymyoglobin (Mb) are the major chromophores in the visible wavelength range. Interestingly, as Hb has four heme prosthetic groups while Mb has only one heme group, the molar extinction coefficient of Hb, is in general, four times greater than that of Mb in the 400–600 nm range. The overlapping of the two inseparable O_2Hb/O_2Mb and Hb/Mb absorption bands centered at 414 nm and 436 nm resulted in the 425 nm peak, and the combination of the three absorption bands at 542 nm, 554 nm and 576 nm resulted in a peak centered at 552 nm [17,18]. It is likely that in healthy living mice, oxygenated proteins O_2Hb/O_2Mb would be predominant (95–100% O_2 saturation in blood), which would diminish the importance of the Hb/Mb absorption peaks. This hypothesis is corroborated by the diffuse reflectance spectra of Caucasian human skin reported by Zonios *et al.*[19] In their study, it was demonstrated that if skin is subjected to

hypoxic conditions, the distinguishable 542 nm and 576 nm absorption peaks decreased in intensity and a new peak centered at 552 nm became evident. Anderson and Parrish also verified that sections of human dermis, free of blood and without a muscle layer, had no indication of absorption peaks in these regions. [12] It must be noted that these peaks are the most intense in the visible spectrum (400–700 nm). In our study, those peaks were significantly higher (~100%) in males than females, regardless of strain. Since the muscle layer had an approximately constant volume among all groups, male mice may possess higher blood content throughout the skin. Riboflavin, flavoproteins and free porphyrins could not be detected in our data.[20]

The absorption bands with peaks at 970 nm, 1190 nm and above 1300 nm occur due to water absorption by resonant molecular vibrations at the O-H bond.[21,22] Above 1350 nm, the water absorption increases strongly and becomes the dominant chromophore. Albino mice had more intense infrared absorption suggesting they had a more hydrated skin. As a consequence of greater absorption by water, albino mice presented the lowest light penetration depth in the best wavelengths for light transmission (1100–1300 nm) in the analyzed spectral region. The minor peak at 1205 nm is due to the presence of lipids.[22,23] In fact, females showed a slightly more pronounced 1205 nm peak (Figure 3a), in agreement with the histological analysis that showed that they had more adipose tissue compared to males (Table 1).

Melanin possesses a high molar extinction coefficient in the ultraviolet region that continuously decays in intensity when moving towards the visible and infrared wavelengths.[24,25] In histology analysis, melanin granules (Figure 4) were found to be restricted to the vicinity of the hair follicles, leaving most of the C57BL/6 skin unpigmented. Yet, no statistically significant difference was found in the presence of melanin between the genders (p=0.27). Nevertheless, the low amount of melanin granules coating the basal epidermal region did not present any appreciable influence in our absorption coefficient data. This fact suggests that melanin is not an important chromophore in depilated skin of C57BL/6 mice.

Both male and female C57BL/6 pigmented mice had on average the same skin thickness (540 ± 20 μm and 540 ± 50 μm, respectively); however, the tissue layers were present in different proportions. The higher abundance of dense connective tissue in males, with anisotropic layers of collagen, contributed to the increased scattering properties of skin from male mice compared to their female counterparts (Figure 3b). [26] It is known that purified fibrous proteins, such as collagen and keratin, are highly scattering materials.[27] Therefore, it can be deduced that connective tissues have stronger scattering properties than adipose tissues due to greater presence of collagen fibers and other fibrous proteins.[28,29] Further studies with isolated tissue layers are necessary to deeply elucidate this interesting finding, but Calabro *et al.* also identified gender as a significant source of variation in optical reflectance measurements in mouse skin *in vivo* and found that variations in the thickness of the dermal layer and in the collagen density were the key variables to explain this observation.[5] Their findings in respect to reflectance and scattering are in good agreement with our observations even though their absorption coefficients differ from ours. This divergence may be explained by disparities of measurement methods. Since the vascular plexus mostly permeates the deeper regions of the highly light-scattering dermis layer,

methods based only on diffuse reflectance measurements may be negatively affected by the variable dermis thickness. On the other hand, the KM model has the limitation of presenting a reduced precision if absorption predominates (*i.e.* μ_a/μ'_s is not <<1). [9,10]

All skin samples analyzed in this study had low attenuation coefficients between 600 and 1350 nm, resulting in this spectral region having the highest values for light penetration depth (Figure 3c,d). This wavelength range is traditionally referred in the literature as the "optical window" due to minimal absorption and scattering by the major biologic tissue components (e.g. heme-proteins, melanin, water, collagen, etc.).[29,28,12] From the lower wavelengths up to 600 nm the different groups had pronounced variation in the reduced attenuation coefficient levels. In general, from 400 nm to 600 nm, absorption is an important component in light-skin interactions, while for the optical window region (600–1350 nm) scattering predominates until absorption predominates again above 1350 nm due to the intense absorption peaks of water.

Although it is a common assumption that wavelengths in the infrared region of the optical window are better suited to optimize the transmission of light in biological tissues, our results show that only a slight increase in transmittance (<10 %) was detected as wavelengths increased from 650 to 1350 nm, and no statistical significant difference was observed (Figure 2b). This same level of variation was observed between experimental groups, at the same wavelength. Therefore, the light transmittance in mouse skin depends, on both the wavelength and the composition of tissue present in the different experimental groups. Thus, it can be suggested that the dosimetry relevant to light-based diagnosis and therapy targeting subcutaneous tissues, depends more on the light attenuation due to different structural features of skin rather than on which precise wavelength is used.

This study provides a solid basis for the optical properties of mice skin among different genders and strains, continuously measured over an extended spectral region. Researchers and technologists can consult our data to provide a basis to design successful animal experimentation. We achieved sufficient precision to distinguish differences among optical properties of male and female mice in pigmented and albino strains. Other investigations using diverse data acquisition and treatment strategies are in good agreement with our results [5,6,30]. Calabro *et al.* carried out *in vivo* experiments using elastic scattering spectroscopy and Monte Carlo simulations and also identified gender and strain as significant sources of variation in the optical properties of mouse skin. The thickness of the dermal layer and the blood content were invoked to explain the variations. Even though they only analyzed a single wavelength (550 nm), the calculated optical coefficients were distributed in a statistically similar manner to the values we obtained and similar divergences were observed between gender and strains, providing corroboration of our analysis.[5]

We must point out that sample preparation is very critical for experimental reproducibility and for comparison with *in vivo* measurements. Sample freshness is a good example of how variations may arise. As far as we know, the impact of sample freshness has never been quantified or reported, but some important points can be inferred. 1) The use of glass slides to position the samples, as we did, can cause mismatched boundary conditions due to Fresnel reflection, which is especially critical for the KM model. We minimized this effect

by moistening the sample surface to reduce refractive index changes. 2) The hydration level of the tissue can cause high variations in both, absorption and scattering, since water is an important tissue chromophore in the infrared region, and it fills the gaps in between tissue microstructures, producing a more homogeneous distribution of refraction index values within the tissue. 3) The oxygenated proteins HbO_2 and MbO_2 rapidly become deoxygenated after blood flow is interrupted in the tissue changing their absorption spectra over time [19]. Within longer periods, the inactivation of a NADH-dependent enzyme – methemoglobin reductase – permits Fe^{+2} present in the heme molecule to be oxidized to Fe^{+3} and this oxidized form can accumulate in sufficient amounts to cause further changes in absorption. 4) Any irritation or damage to the skin while shaving or depilating the mice would affect results negatively. [7]

A limitation of the KM model is that it could introduce some imprecision to our calculation of coefficients since it assumes matched boundary conditions (*i.e.*, the same refractive index between propagating media) and that scattering is predominant over absorption. [9, 11, 13] However, it has been demonstrated that the KM coefficients can provide acceptable approximations for μ_s' μ_a, and δ (equations 5–8), if scattering is predominant. [9, 11, 13] As a precautionary measure, we minimized mismatched boundary conditions by moistening the skin surface to exclude air from the interface and create a gradually increasing refractive index between samples and glass ($N_{\text{biological tissues}}$ 1.35–1.45, $N_{\text{water}} = 1.33$ and $N_{\text{glass}} = 1.46$). Overall, our results suggest that KM can provide a reliable analytical model of photon transport to obtain optical properties of *ex vivo* biological tissues analyzed spectroscopically with a single integrating sphere. All major absorption peaks were clearly distinguished and scattering curves behaved, as expected, with continuous exponential decays as a function of wavelength and presented minor deformations in regions of high absorption peaks (Fig. 3a,b). Other robust theoretical models generally require complex computational simulations (*e.g.* Monte Carlo simulations) to report optical properties of turbid media in terms of the same optical coefficients (μ_s' μ_a and δ). [9, 11]

The edge loss at the ports of integrating spheres could also affect our absorption coefficients, producing higher values than actually expected. These edge losses are wavelength dependent and are most important where absorption is minimal but scattering is still relevant, as in the optical window. Since our samples were not inserted into the sphere, light scattering at 90° degrees could attenuate transmission and be mistakenly interpreted as absorption. We tried to compensate for this problem using a small beam diameter (<0.5 mm) to keep the lateral propagation width ($1/(\mu_a + \mu_s')$) much smaller than the integrating sphere port diameter (~20 mm). Theoretically, this artifact could deviate the measured μ_a up to values as much as 10-fold higher than the true μ_a. In fact, in the optical window region our absorption results exceeded up to 7 times the measurements made by Jacques using rats (rather than mice), while our reduced scattering values were 4 to 10 times lower [11, 30]. But alternatively, such differences may also be explained due to greater abundance of light-scattering fibrous proteins in the thicker epidermis and dermis of rats, when compared to thinner skin of mice, illustrating the diversity of tissue optics in different animal models.

Fluorescent molecular probes and genetically engineered bioluminescent microorganisms and cancer cells have been widely used in studies to non-invasively monitor biological

phenomena *in vivo* and, in fact, much relevant knowledge has been developed based on these techniques. [31,32] However, the emission wavelengths of bioluminescence are commonly between 400 and 600 nm where, according to our data, high absorption and diffuse scattering occurs in the skin tissue. Curtis et al. reported, that as C57BL/6 mice age, the melanin concentration in the skin increases affecting optical bioluminescence quantitation. [6] Indeed, when a weak bioluminescent emission is located underneath any tissue this may lead to low signal detection and relatively more blurred images are obtained decreasing the accuracy of the technique. The same situation can be observed in fluorescence optical imaging where short wavelength fluorescent probes are employed for observing subcutaneous targets. [6, 31, 32]

With regard to optical techniques involving signal detection or imaging in deep tissues, such as optical coherence tomography or multiphoton fluorescence microscopy, our study showed interesting findings. For all evaluated wavelengths, female mice exhibited higher light penetration depths compared to their male counterparts, with females from C57BL/6 strain always showing the greatest values (average ± SEM, Figure 3d). The difference in penetration depth between pigmented and albino males reaches up to 500 μm, and to 700 μm when comparing females from both strains. This affirmation is valid for λ= 1100 nm, which is the wavelength that presented the highest δ (Figure 3d), and also is in the spectral range of many biomedical light sources, whose emission is designed for deep penetration. [1, 4, 28] Supposing the investigated target of analysis is located beneath the skin, researchers should perhaps choose the C57BL/6 strain over albino mice, since the differences in penetration depth can occasionally be larger than their skin thickness (Table 1). Therefore, the reported optical coefficients can be used to facilitate development and optimize the outcomes of many biophotonics technologies used in therapeutics, surgery, diagnosis and luminescence detection in biomedicine. However, we also propose that investigations on differences between the optical properties of skin from mouse and other animal models, or between human skin, using the same methods, could be an interesting approach to facilitate development of translational biophotonic technologies based on tissue optics.

4. Conclusion

This study used easily reproducible methods to report comprehensive fundamental measurements of light interactions with mice skin with wide applicability in biophotonics. Within a broad wavelength range (400–1400 nm) all main optical properties of visible and near infrared radiation could be inferred. Optical property differences between males and females of pigmented and albino strains were found to be significant. Gender mostly affects mouse skin optical properties in the visible range due to variations in blood and dense connective tissue abundance, while pigmented and albino strains can introduce more variations due to the hydration level of the skin, leading to absorption variations in the infrared spectral region. Melanin, however, only accumulates in small quantities around hair follicles and does not introduce major optical variations. Our results stress the importance of considering the mouse strain and gender to plan pre-clinical experiments that are dependent on light-skin interactions.

Acknowledgments

Authors gratefully recognize the efforts made on histological processing by Cristiano de Loura Santana and Fabiana dos Santos from the Biophotonics Applied to Health Sciences Laboratory at Nove de Julho University (Uninove). The financial support was provided by the Brazilian funding agencies FAPESP (grant 2014/02564-1) and CNPq. MR Hamblin was supported by US NIH grant R01AI050875.

References

1. Anderson RR. Lasers for dermatology and skin biology. J. Invest. Dermatol. 2013; 133:E21–E23. [PubMed: 23820722]
2. França CM, França CM, Núñez SC, Prates RA, Noborikawa E, Faria MR, Ribeiro MS. Low-intensity red laser on the prevention and treatment of induced-oral mucositis in hamsters. J. Photochem. Photobiol. B. 2009; 94:25–31. [PubMed: 18976931]
3. Panchenko PA, Sergeeva AN, Fedorova OA, Fedorov YV, Reshetnikov RI, Schelkunova AE, Grin MA, Mironov AF, Jonusauskas G. Spectroscopical study of bacteriopurpurinimide-naphthalimide conjugates for fluorescent diagnostics and photodynamic therapy. J. Photochem. Photobiol. B. 2014; 133:140–144. [PubMed: 24727406]
4. Sroka R, Stepp H, Hennig G, Brittenham GM, Rühm A, Lilge L. Medical laser application: translation into the clinics. J. Biomed. Opt. 2015; 20:061110. [PubMed: 26079966]
5. Calabro K, Curtis A, Galarneau JR, Krucker T, Bigio IJ. Gender variations in the optical properties of skin in murine animal models. J. Biomed. Opt. 2011; 16:8.
6. Curtis A, Calabro K, Galarneau JR, Bigio IJ, Krucker T. Temporal variations of skin pigmentation in C57BL/6 mice affect optical bioluminescence quantitation. Mol. Imag. Biol. 2011; 13:1114–1123.
7. Sabino CP, Meneguzzo DT, Benetti E, Kato IT, Prates RA, Ribeiro MS. Red laser attenuation in biological tissues: study of the inflammatory process and pigmentation influence. Proceed. SPIE. 2012; 8211:821105.
8. Yarborough JM. Taking the confusion out of matching medical lasers to applications. Photon. Spect. 1992; 26:88.
9. Jacques SL, W Pogue B. Tutorial on diffuse light transport. J. Biomed. Opt. 2008; 13:19.
10. Kubelka P, Munk F. Ein beitrag zür optik der farbanstriche. Z. Techn. Phys. 1931; 12:593–601.
11. Cheong WF, Prahl SA, Welch AJ. A review of the optical properties of biological tissues. IEEE J. Quantum Electron. 1990; 26:2166–2185. An updated version is available online at http://omlc.org/~prahl/pubs/pdfx/cheong90a.pdf.
12. Anderson RR, Parrish JA. The optics of human skin. J. Invest. Dermatol. 1981; 77:13–19. [PubMed: 7252245]
13. Thennadil SN. Relationship between the Kubelka-Munk scattering and radiative transfer coefficients. J Opt Soc Am A. 2008; 25:1480–1485.
14. Rasband, WS. [acessed: 08, 2014] ImageJ. http://imagej.nih.gov/ij/
15. Lillie RD, Donaldson PT, Vacca LL, Pizzolato PP, K Jirge S. Reduction and azo coupling of quinones. A histochemical study of human cutaneous melanin and adrenochrome. Histochem. 1977; 51:141–152.
16. Azzi L, El-Alfy M, Martel C, Labrie F. Gender differences in mouse skin morphology and specific effects of sex steroids and dehydroepiandrosterone. J Invest Dermatol. 2005; 124:22–27. [PubMed: 15654949]
17. Millar SJ, W Moss B, Stevenson MH. Some observations on the absorption spectra of various myoglobin derivatives found in meat. Meat Sci. 1996; 42:277–288. [PubMed: 22060775]
18. Prahl, S. [accessed: 06, 2015] Optical absorption of hemoglobin. http://omlc.org/spectra/hemoglobin/
19. Zonios G, Bykowski J, Kollias N. Skin melanin, hemoglobin, and light scattering properties can be quantitatively assessed in vivo using diffuse reflectance spectroscopy. J. Invest. Dermatol. 2001; 117:1452–1457. [PubMed: 11886508]
20. Prahl, S. [accessed: 06, 2015] PhotochemCAD Chemicals. http://omlc.org/spectra/PhotochemCAD/index.html

21. Silva DFT, Mesquita-Ferrari RA, Fernandes KPS, Raele MP, Wetter NU, Deana AM. Effective transmission of light for media culture, plates and tubes. Photochem. Photobiol. 2012; 88:1211–1216. [PubMed: 22540924]
22. Tsai CL, Chen JC, Wang WJ. Near-infrared absorption property of biological soft tissue constituents. J. Med. Biol. Eng. 2001; 21:7–14.
23. Bashkatov AN, Genina EA, Kochubey VI, Kochubey VI, Tuchin VV. Optical properties of human skin, subcutaneous and mucous tissues in the wavelength range from 400 to 2000 nm. Opt. Spectrosc. 2005; 99:836–842.
24. Jacques SL, McAuliffe DJ. The melanosome: threshold temperature for explosive vaporization and internal absorption coefficient during pulsed laser irradiation. Photochem. Photobiol. 1991; 53:769–775. [PubMed: 1886936]
25. Nielsen KP, Zhao L, Juzenas P, Stamnes JJ, Stamnes K, Moan J. Reflectance spectra of pigmented and nonpigmented skin in the UV spectral region. Photochem. Photobiol. 2004; 80:450–455. [PubMed: 15623329]
26. Wu SL, Li H, Yang HQ, Zhang X, Li Z, Xu S. Quantitative analysis on collagen morphology in aging skin based on multiphoton microscopy. J. Biomed. Opt. 2011; 16:040502. [PubMed: 21529064]
27. Millington KR. Diffuse reflectance spectroscopy of fibrous proteins. Amino Acids. 2012; 43:1277–1285. [PubMed: 22218994]
28. Bashkatov AN, Genina EA, Kochubey VI, Kochubey VI, Tuchin VV. Optical properties of human skin, subcutaneous and mucous tissues in the wavelength range from 400 to 2000 nm. J. Phys. D-Appl. Phys. 2005; 38:2543–2555.
29. Jacques SL. Optical properties of biological tissues: a review. Phys. Med. Biol. 2013; 58:R37–R61. [PubMed: 23666068]
30. Jacques S. Personal Communication. 1993
31. Close DM, Xu TT, Sayler GS, Ripp S. In vivo bioluminescent imaging (BLI): noninvasive visualization and interrogation of biological processes in living animals. Sensors. 2011; 11:180–206. [PubMed: 22346573]
32. Silva ZS Jr, Bussadori SK, Fernandes KP, Huang YY, Hamblin MR. Animal models for photodynamic therapy (PDT). Biosci Rep. 35:e00265. [PubMed: 26415497]

- We present μ_a, μ'_s, μ'_t and δ of albino and pigmented mice skin from both genders, from 400 to 1400 nm;
- Dense connective tissues are more abundant in males and present strong scattering;
- Males present stronger absorption by heme-proteins indicating higher blood content;
- Albino mice present more intense infrared absorption due to higher water content;
- Melanin in depilated pigmented mouse skin is irrelevant for light absorption.

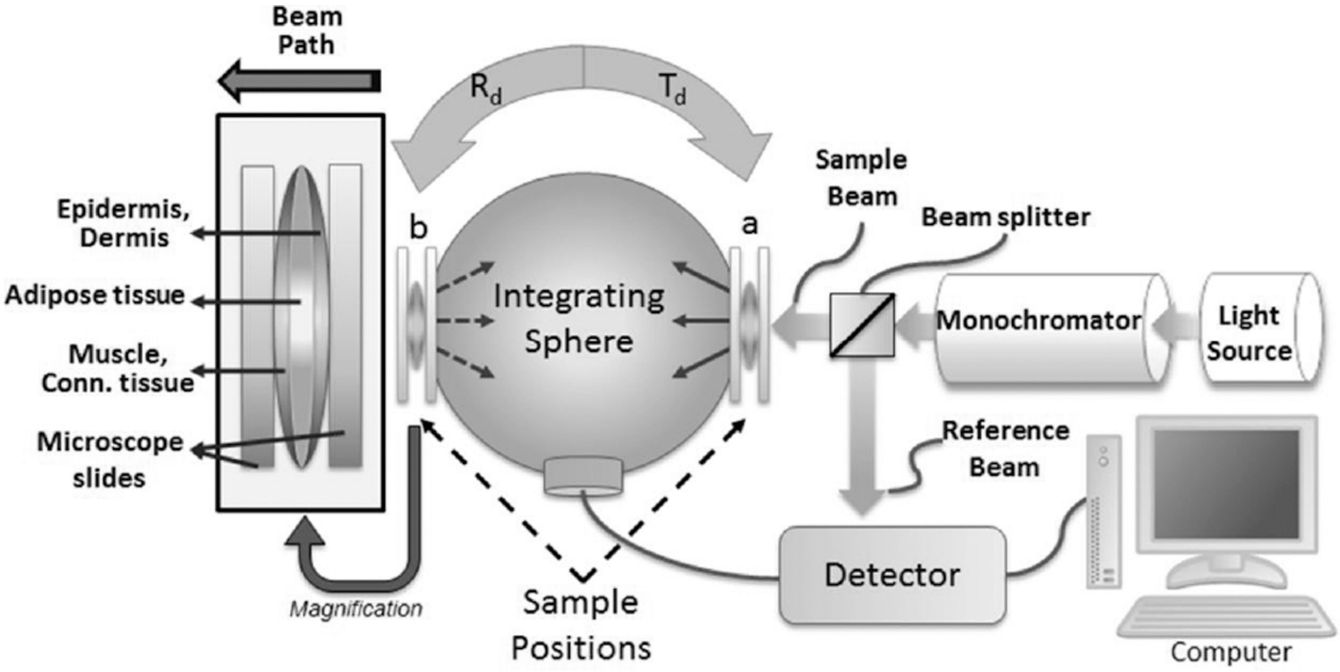

Figure 1.

Schematic diagram of the commercial spectrometer system coupled to a single integrating sphere. To provide mechanical support, each sample was placed in between two glass microscopy slides. The transmittance spectra were obtained by placing the sample at position “a” with port “b” closed, and reflectance spectra were acquired shifting the sample to position “b”. For all measurements, the sample beam was directed in the epidermis-dermis direction.

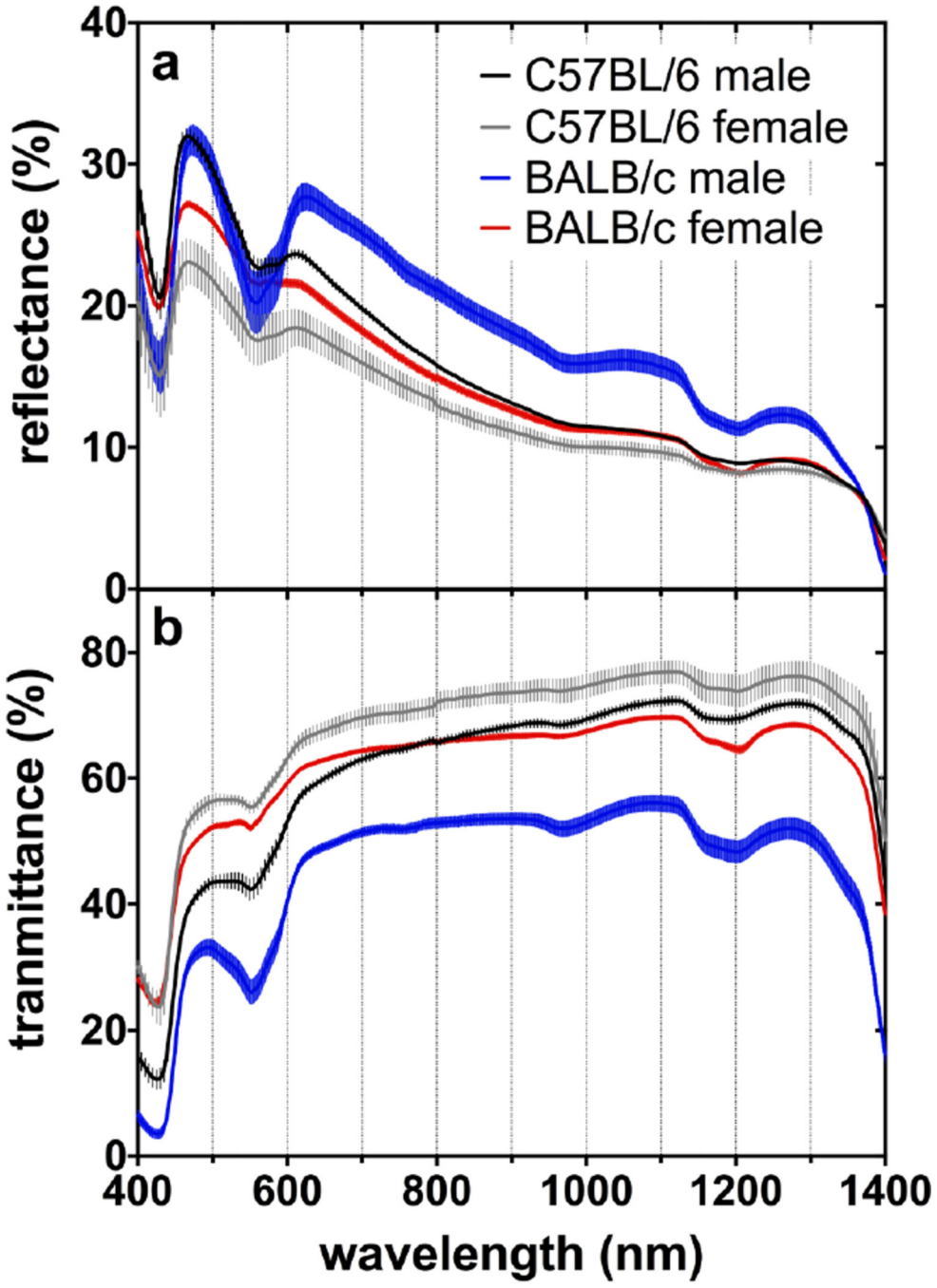

Figure 2.
Average and SEM of (a) diffuse reflectance and (b) diffuse transmittance versus wavelength.

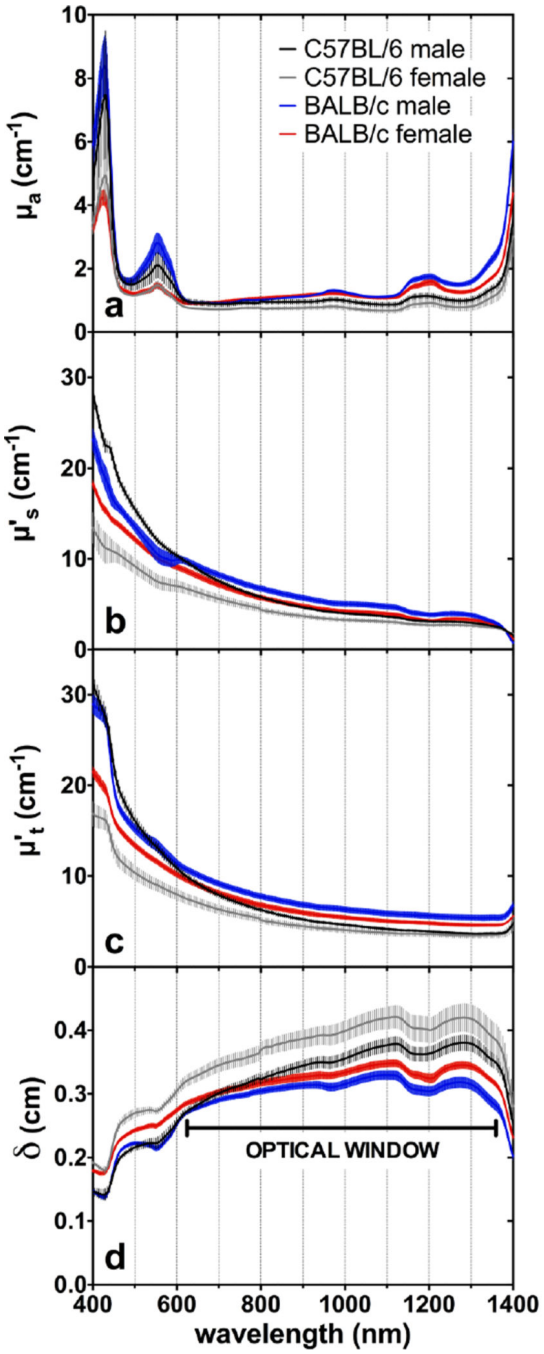

Figure 3.

Average and SEM of (a) Absorption, (b) reduced scattering, (c) reduced attenuation coefficients and (d) penetration depth versus wavelength. The maxima penetration depth at (d) represents the “optical window” for light penetration into depilated mice skin.

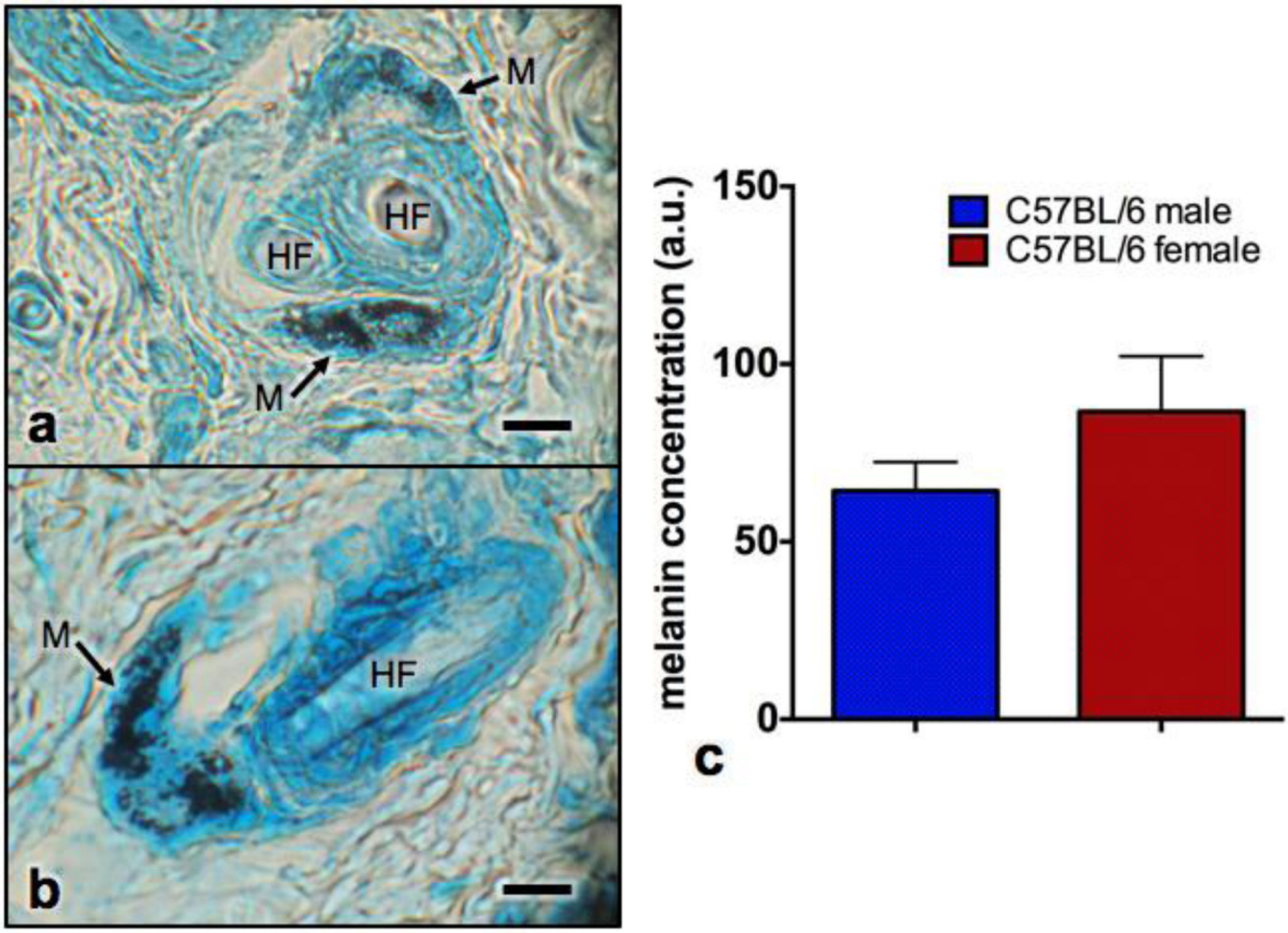

Figure 4.

Photomicrograph of the (a) transversal and (b) longitudinal aspect of a primary hair follicle stained with Lillie's stain. Note the hair follicle (HF) and melanin granules (arrows) seen as round black structures. (c) Melanin concentrations in male and female C57BL/6 mice skin presented in arbitrary units of melanin granule area, averages and standard errors (n=5 per group). Scale bar corresponds to 20 μm.

Table 1

Mean and SEM values of the thickness of epidermis, dermis, adipose tissue and muscle layer quantified by histology.

	BALB/c		C57BL/6	
	Female	**Male**	**Female**	**Male**
Epidermis	12.08 ± 3.14	10.19 ± 3.29	13.08 ± 3.50	12.53 ± 3.97
Dermis	156.65 ± 55.23	343.44 ± 100.09	162.02 ± 15.12	226.33 ± 36.86
Adipose tissue	168.01 ± 52.31	40.17 ± 9.65	189.37 ± 64.14	103.05 ± 61.24
Muscle	91.68 ± 21.95	90.47 ± 51.96	83.34 ± 27.14	90.53 ± 18.23